Plume height, volume, and classification of explosive volcanic eruptions based on the Weibull function

Bonadonna, Costanza; Costa, Antonio

Bull Volcanol (2013) 75:742
DOI 10.1007/s00445-013-0742-1

RESEARCH ARTICLE

Plume height, volume, and classification of explosive volcanic eruptions based on the Weibull function

Costanza Bonadonna · Antonio Costa

Received: 30 January 2013 / Accepted: 10 June 2013

Abstract The Weibull distribution between volume and square root of isopach area has been recently introduced for determining volume of tephra deposits, which is crucial to the assessment of the magnitude and hazards of explosive volcanoes. We show how the decay of the size of the largest lithics with the square root of isopleth area can also be well described using a Weibull function and how plume height correlates strongly with corresponding Weibull parameters. Variations of median grain size (Mdϕ) values with square root of area of the associated contours can be, similarly, well fitted with a Weibull function. Weibull parameters, derived for both the thinning of tephra deposits and the decrease of grain size (both maximum lithic diameter and Mdϕ), with a proxy for the distance from vent (e.g., square root of isoline areas) can be combined to classify the style of explosive volcanic eruptions. Accounting for the uncertainty in the derivation of eruptive parameters (e.g., plume height and volume of tephra deposits) is crucial to any classification of eruptive style and hazard assessment. Considering a typical uncertainty of 20 % for the determination of plume height, a new eruption classification scheme based on selected Weibull parameters is proposed. Ultraplinian, Plinian, Subplinian, and small–moderate explosive eruptions are defined on the ground of plume height and mass eruption rate. Overall, the Weibull fitting represents a versatile and reliable strategy for the estimation of both the volume of tephra deposits and the height of volcanic plumes and for the classification of eruptive style. Nonetheless, due to the typically large uncertainties (mainly due to availability of data, compilation of isopach and isopleth maps, and discrepancies from empirical best fits), plume height, volume, and magnitude of explosive eruptions cannot be considered as absolute values, regardless of the technique used. It is important that various empirical and analytical methods are applied in order to assess such an uncertainty.

Keywords Tephra · Maximum clast · Mdϕ · Uncertainty · Eruptive style · Explosive eruptions

Editorial responsibility: J.E. Gardner

Electronic supplementary material The online version of this article (doi:10.1007/s00445-013-0742-1) contains supplementary material, which is available to authorized users.

C. Bonadonna (✉)
Department of Earth Sciences, University of Geneva,
Geneva, Switzerland
e-mail: Costanza.Bonadonna@unige.ch

A. Costa
Istituto Nazionale di Geofisica e Vulcanologia, Sezione di Bologna,
Bologna, Italy

Introduction

Progress in physical volcanology relies on the identification and analysis of common features of eruptions having similar characteristics (Walker 1973). Furthermore, the possibility of comparing the scale or magnitude of eruptions at a same volcano, or at different volcanic systems, is necessary to characterize historic volcanism and for the compilation of hazard assessment and potential activity scenarios for future events (Newhall and Self 1982). Walker (1980) introduced five parameters ("bigness") for the estimation of the scale of explosive eruptions: (1) magnitude (volume of erupted material typically converted to dense rock equivalent (DRE)); (2) intensity (volume of ejecta per unit time); (3) dispersive power (related to the total area of dispersal and, therefore, to plume height); (4) violence (related to kinetic energy); (5) destructive potential (related to the extent of devastation). The characterization and classification of explosive eruptions is based on parameters mostly derived from studies of tephra deposits, namely plume height, bulk erupted volume (deposit volume), DRE (volume of dense, unvesiculated magma), magnitude, mass eruption rate, destructiveness index, magnitude and intensity scale, dispersal index (D), fragmentation index (F), thickness half distance (b_t), clast

Published online: 25 July 2013

half distance (b_c), which are somehow related to the five parameters highlighted by Walker (1980) (e.g., Walker 1973; Newhall and Self 1982; Pyle 1989, 2000; Mason et al. 2004; Cioni et al. 2008).

A classification based on tephra deposits is made possible by the fact that tephra generation and sedimentation is strongly related to eruptive dynamics (e.g., volume of erupted magma, magma fragmentation, and plume height) and, therefore, first-order tephra deposit features (e.g., thickness and grain size) are likely to follow well-defined variation trends with distance from vent (e.g., Pyle 1989). However, these variation trends are typically captured by empirical models (e.g., exponential and power law fit for the description of thickness data) that strongly depend on data availability as well as on the strategies used to produce these data (e.g., averaging techniques for the determination of maximum clast size and median diameter). Eruption classification and characterization are then naturally associated with large uncertainties related both to deposit exposure and to the models used to describe tephra deposits (Bonadonna and Costa 2013). As an example, Biass and Bonadonna (2011) have shown how the same eruptions could be classified as either Plinian or Subplinian, depending on the technique used to characterize the largest clasts. Likewise Longchamp et al. (2011) have shown that different values for Volcanic Explosivity Index (VEI) could be assigned to two Nisyros eruptions, depending on the model used to determine the erupted volume. Nonetheless, existing classification schemes are strongly deterministic, often generating interesting debates on the boundaries between eruptive styles and on the way eruptions should be best classified (e.g., Walker 1973, 1980; Pyle 1989; Sparks et al. 1992). Considering that uncertainty is intrinsic to the description of any natural system, explosive eruptions would be better characterized if uncertainties were accurately described and accounted.

We propose new classification schemes that account for the uncertainties associated with the determination of both eruptive parameters and tephra-fall deposit features and that are based on a general distribution that best describes variation trends of both thickness and grain size with distance from vent, namely the Weibull distribution. Such a distribution was already proposed by Bonadonna and Costa (2012) as an alternative way to fit thickness data and determine erupted volume, reconciling the debate on the use of exponential versus power law correlations.

Thickness variations of tephra fall deposits

Several empirical strategies have been proposed to describe the thinning of tephra deposits, including two segments on a log–log plot, the trapezoidal rule, and the more recent methods based on the exponential and power law thinning on a semilog plot (see Fierstein and Nathenson (1992), Bonadonna and Houghton (2005), and Gonzalez-Mellado and De la Cruz-Reyna (2010) for a review). The empirical fit of one or a few straight exponential segments on a semi-log plot (Fierstein and Nathenson 1992, 1993; Pyle 1989, 1995) better fits natural deposits and is based on some geological observations that, as a trend, both thickness and grain size decay exponentially with distance from the vent (e.g., Thorarinsson 1954; Walker 1980). Nonetheless, the exponential integration, first introduced by Pyle (1989), generated a large debate around the significance of the method as it was suggested that such a strategy can significantly underestimate the volume when the distal data are missing (Fierstein and Nathenson 1992; Rose 1993; Pyle 1995). In fact, more recent studies have shown that well-preserved tephra deposits do not necessarily follow an exponential decay as distal ash might settle differently (e.g., Bonadonna et al. 1998; Rose and Durant 2009).

The power law (PL) fit or at least three exponential segments on a semi-log plot (Bonadonna and Houghton 2005) were introduced to describe better the thinning of well-preserved deposits and the results of numerical investigations that show a much more gradual thinning than predicted by the one or two exponential segments, especially for eruptions that produce a large amount of volcanic ash as well as lapilli-sized particles (Bursik et al. 1992; Sparks et al. 1992; Rose 1993; Bonadonna et al. 1998). Nonetheless, three segments cannot always be identified, especially for poorly preserved deposits, and the PL fit has problems in defining the integration limits (as it cannot be integrated between zero and infinity). In fact, depending on the data distribution and the thinning trend, the resulting PL volume is very sensitive to the proximal or the distal integration extreme for small (i.e., PL exponent >2) and large deposits (i.e., PL exponent <2), respectively (Bonadonna and Costa 2013).

Sulpizio (2005) presented three empirical methods for the calculation of distal volumes based on the information retained by the proximal deposit (up to thickness >1 cm), as also partially suggested by Koyaguchi (1996) and Legros (2000). In particular, he suggested (1) the compilation of distal isopachs in the case of sparse distal data assuming same elliptical shape (same eccentricity) and same dispersal axis of proximal isopachs; (2) the empirical determination of a break-in-slope between proximal and distal data in case only one distal isopach line is available; and (3) the empirical calculation of distal thinning when only proximal data are available. These three techniques give good agreement with field data for the 30 deposits used in his case study. Nonetheless, due to the difficulty of extrapolating proximal patterns to distal areas, the application of all these methods to poorly preserved deposits is not always straightforward, in particular in cases when the wind patterns in proximal and distal area are significantly different (e.g., Costantini et al.

2009; Longchamp et al. 2011). Pyle (1999) and Legros (2000) developed a strategy to estimate erupted volumes when only one proximal isopach line can be defined based on the available data. Such a method gives estimated minimum volumes of the same order of magnitude as only the first one or two segments on semi-log plots of thickness versus square root of the area were available.

Bonadonna and Costa (2012) have introduced the use of the Weibull distribution for the integration of the log of thickness, T, data versus square root of isopach areas, x, to reconcile the debate on the use of the exponential and PL fitting:

$$T = \theta_{\text{th}} \left(\frac{x}{\lambda_{\text{th}}}\right)^{n_{\text{th}}-2} \exp\left[-\left(\frac{x}{\lambda_{\text{th}}}\right)^{n_{\text{th}}}\right] \quad (1)$$

with λ_{th}, θ_{th}, and n_{th} being empirically determined parameters that will be discussed below. Relationship (1) can be used to calculate the volume, V, as function of the square root of isopach area $x = \sqrt{A}$:

$$\begin{aligned} V(x) &= \int_0^x T\mathrm{d}A = 2\int_0^x T(s)\mathrm{sds} \\ &= \frac{2\theta_{\text{th}}\lambda_{\text{th}}^2}{n_{\text{th}}} \int_0^x \frac{n_{\text{th}}}{\lambda_{\text{th}}} \left(s \middle/ \lambda_{\text{th}}\right)^{n_{\text{th}}-1} e^{-\left(\frac{s}{\lambda_{\text{th}}}\right)^{n_{\text{th}}}} \mathrm{ds} \\ &= \frac{2\theta_{\text{th}}\lambda_{\text{th}}^2}{n_{\text{th}}} \left[1 - e^{-\left(\frac{x}{\lambda_{\text{th}}}\right)^{n_{\text{th}}}}\right] \end{aligned} \quad (2)$$

that shows how $V(x)$ is described by a Weibull distribution. Integrating Eq. (2) from zero to infinity, we obtain the total volume as:

$$\begin{aligned} V &= \int_0^\infty T\mathrm{d}A = 2\int_0^\infty T(x)x\mathrm{d}x = \frac{2\theta_{\text{th}}\lambda_{\text{th}}^2}{n_{\text{th}}} \left[1 - e^{-\left(\frac{x}{\lambda_{\text{th}}}\right)^{n_{\text{th}}}}\right]_0^\infty \\ &= \frac{2\theta_{\text{th}}\lambda_{\text{th}}^2}{n_{\text{th}}} \end{aligned} \quad (3)$$

The Weibull distribution can be considered as a generalization of the exponential distribution, but it has the advantage to capture the variation in thinning rate that, in contrast to the exponential distribution, can change with distance, and therefore, it can better reproduce the natural curvature of deposit thinning. By varying the characteristic values of the shape parameter n_{th}, the Weibull distribution can model a wide variety of distributions, ranging from the exponential distribution for $n_{\text{th}}=1$, to the Rayleigh distribution for $n_{\text{th}}=2$, to the normal distribution for n_{th} between 3 and 4, and to the log-normal distribution for various values of n_{th} (Brown and Wohletz 1995). With respect to the PL fit, the Weibull distribution can be integrated between zero and infinity, reducing the uncertainty in volume estimation. Bonadonna and Costa (2012) have shown how the uncertainties of volume estimation associated with the use of the Weibull integration are smaller than those associated with the exponential integration, and that the Weibull distribution can better capture the deposit thinning when proximal, medial, or distal data are missing. It has also to be considered that the uncertainties associated with the multiple exponential segment method can be underestimated when the number of points used to characterize each segment is small (e.g., the most drastic case is when each segment is determined by two points only). Finally, as mentioned earlier, the Weibull distribution can reproduce the gradual thinning as also reproduced by the power law regression, but it is associated with smaller uncertainties with respect to the PL integration when proximal (for small deposit; VEI $\leq$3; PL exponent >2) and distal (for large deposits; VEI >3; PL exponent <2) data are missing. Moreover, as we show in the Appendix 1, the Weibull distribution for tephra deposits can be heuristically derived, generalizing the basic physical model proposed by Bursik et al. (1992), Sparks et al. (1992), Bonadonna and Phillips (2003), and Bonadonna et al. (2005).

Grain size variations of tephra fall deposits

In addition to the total erupted mass and the thinning of tephra deposits, the general characteristics of the initial grain size population also give vital information on the dynamics and style of explosive eruptions. Once particles are ejected from the vent, they will sediment away from the source based mainly on the height of the plume, on the surrounding wind field and on their aerodynamics features. Like deposit thickness, particle size also seems to be characterized by a systematic decrease with distance from vent, shown by the values of both maximum clast and median particle diameter (commonly expressed in phi-unit, a logarithmic unit used to measure grain sizes with $\phi = -\log_2 D$, where D is the particle diameter in millimeter). Nonetheless, the associated decreasing trend and/or decreasing rate are not always equal for pumices, lithics, and Mdϕ (e.g., Thorarinsson 1954; Walker 1980; Pyle 1989). These variations in decreasing rate could be due to variable lithic content, particle density, and sorting as particles with different aerodynamics properties result in different sedimentation patterns (Pyle 1989). In addition, isopleth maps are typically more circular than isopach maps because the size of large clasts decreases upwind and downwind at a similar rate.

Decrease of lithic size (ML) with distance from vent, i.e., ML vs square root of isopleth area, follows a Weibull trend

described by Weibull parameters λ_{ML}, θ_{ML}, and n_{ML} (Fig. 1 and Table 1) as:

$$ML = \theta_{ML}\left(\frac{x}{\lambda_{ML}}\right)^{n_{ML}-2}\exp\left[-\left(\frac{x}{\lambda_{ML}}\right)^{n_{ML}}\right] \quad (4)$$

In this paper, we did not consider the decreasing trend of pumice size (MP) due to the high probability of breakage upon impact with the ground (e.g., Walker 1980; Sparks et al. 1981; Bonadonna et al. 2013). Typically, the datasets describing the decrease of the largest lithics and pumices are smaller than the deposit-thinning datasets due to the difficulty of measuring the diameters of small particles in the field. As a result, ML datasets range from 0.4 to 100 cm and most typically within 0.8–10 cm. These small datasets cannot describe the sedimentation trend of all size classes associated with a given eruption and are more difficult to interpret than deposit-thinning trends. Nonetheless, the Weibull provides a robust method for the description of such a trend (Fig. 1, Table 1; Appendix Table 4).

Given the difficulty of collecting and analyzing the largest clasts of any given outcrop, we consider the decrease of Mdϕ with distance from vent as a robust alternative. Mdϕ is here defined as median grain size in Inman (1952; Mdϕ=ϕ50) expressed in centimeters. Unfortunately, isogrades showing the distribution of Mdϕ with distance from vent are available only for a few cases (e.g., Hatepe, Waimihia (Walker 1981a); Taupo (Walker 1980); Tarawera (Walker et al. 1984); Pululagua (Volentik et al. 2010); Cotopaxi layers 3 and 5 (Tsunematsu 2012; Table 1). Weibull fitting seems promising also for the description of the Mdϕ variation with distance from vent (Fig. 2):

$$Md\phi = \theta_{Md\phi}\left(\frac{x}{\lambda_{Md\phi}}\right)^{n_{Md\phi}-2}\exp\left[-\left(\frac{x}{\lambda_{Md\phi}}\right)^{n_{Md\phi}}\right] \quad (5)$$

where $\lambda_{Md\phi}$ $\theta_{Md\phi}$, and $n_{Md\phi}$ are the associated Weibull parameters.

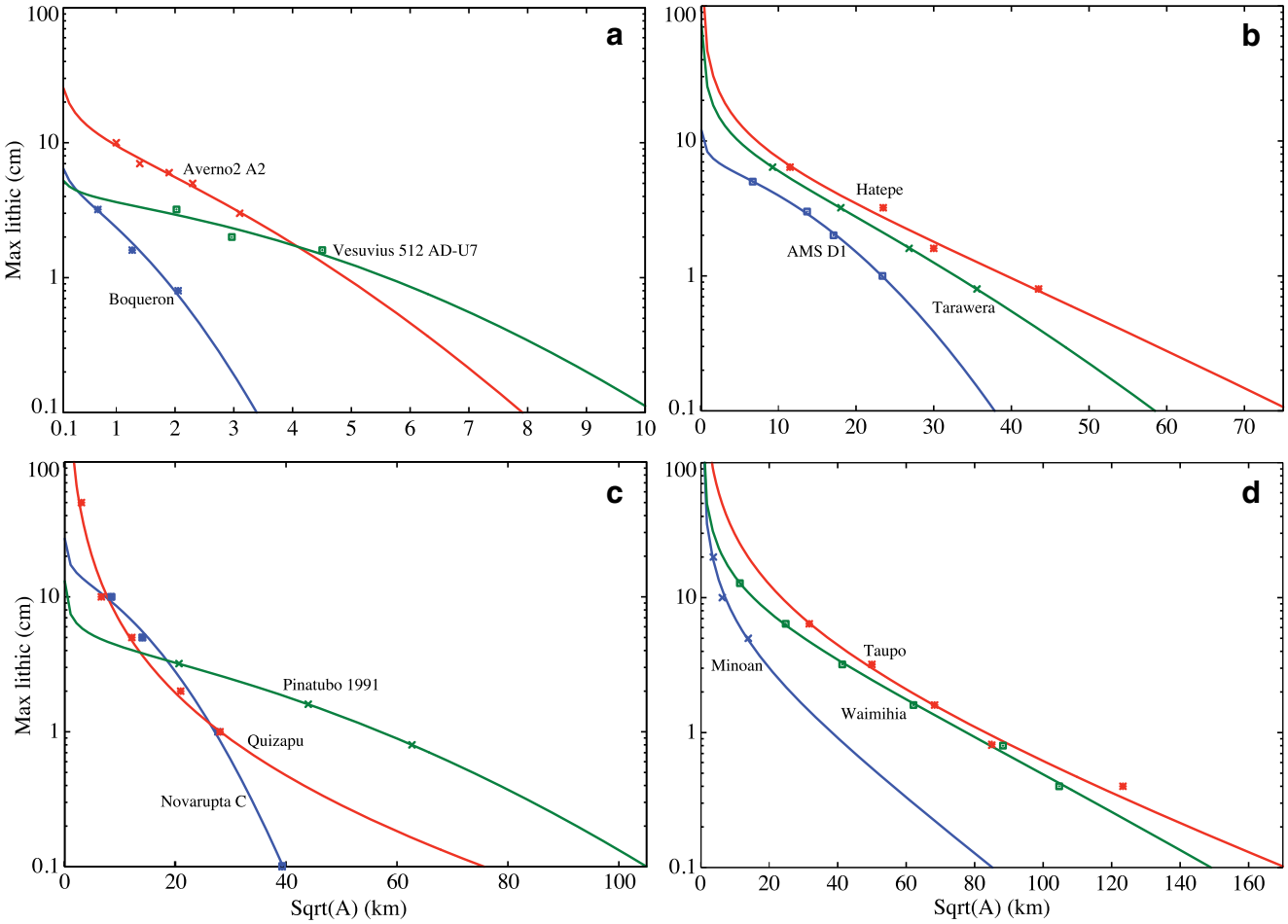

Fig. 1 Semi-log plots of square root of isopleth area (in kilometers) versus lithic clast size (in centimeters) showing the Weibull best fit for various deposits of: **a** VEI 3, **b** VEI 4, **c** VEI 5, **d** VEI 6

Table 1 Eruption parameters. Main parameters associated with the eruptions considered in our study

#	Eruption	Volume (km^3)	λ_{th} (km)	λ_{ML} (km)	$\lambda_{Md\phi}$ (km)	$\lambda_{ML}/\lambda_{th}$	$\lambda_{Md\phi}/\lambda_{th}$	Ht (km)	Ht* (km)	Ht** (km)
1	Vesuvius 512 (U7)	0.008	2.5	5.4		2.1		9.0	12.6	
2	Averno2-A1	0.002	1.8	2.3		1.3		8.0	7.9	
3	Averno2-A3	0.006	1.1	2.0		1.9		9.0	7.4	
4	Averno2-A4	0.009	1.0	4.4		4.4		9.0	11.3	
5	Averno2-A5	0.003	1.5	2.2		1.4		9.0	7.7	
6	Averno2-A2	0.019	3.1	3.4		1.1		10.0	9.9	
7	Boqueron C	0.018	2.4	2.7		1.1		7.0	8.6	
8	Vesuvius 512 (U5top)	0.013	5.6	7.9		1.4		15.0	15.6	
9	Montaña Blanca	0.077	23.6	6.2		0.3		12.0	13.6	
10	El Chichon A	0.170	30.9	31.3		1.0		27.0	33.3	
11	Fogo A	0.300	19.0	17.6		0.9		26.0	24.3	
12	Fogo 1563	0.642	13.8	12.0		0.9		17.5	19.7	
13	Agnano M Spina (B1)	0.167	18.2	25.2		1.4		23.0	29.5	
14	Cotopaxi L3	0.541	15.7	15.3	23.5	1.0	1.5	23.0	22.4	24.9
15	Agnano M Spina (D1)	0.215	29.7	18.3		0.6		27.0	24.8	
16	Cotopaxi L5	0.230	13.6	17.0	19.2	1.3	1.4	26.0	23.8	22.5
17	Hatepe 186 AD	0.656	44.8	32.0	58.9	0.7	1.3	35.0	33.7	39.8
18	Tarawera 1886	0.472	19.8	25.7	42.9	1.3	2.2	33.0	29.8	33.9
19	Pululagua 2450BP	0.319	21.9	24.8	30.4	1.1	1.4	27.0	29.3	28.4
20	Fontana Lapilli E	1.900	83.7	16.8		0.2		27.0	23.6	
21	Fontana Lapilli F	1.900	83.7	14.6		0.2		29.0	21.9	
22	Novarupta A 1912	9.044	150.7	12.3		0.1		26.0	19.9	
23	Novarupta C 1912	2.614	62.6	17.2		0.3		25.0	24.0	
24	Novarupta F 1912	7.787	245.5	12.6		0.1		23.0	20.2	
25	Quizapu 1932	9.037	256.7	26.6		0.1		27.0	30.5	
26	Santa Maria 1902	7.952	119.1	16.8		0.1		27.0	23.7	
27	Pinatubo 1991	3.000	229.6	53.8		0.2		40.0	44.8	
28	Minoan 3.6 ka BP	38.60	322.5	36.5		0.1		36.0	36.2	
29	Taupo 186 AD	12.00	155.9	56.8[a]	68.1	0.4	0.4	50.0	46.2	42.9
30	Waimihia	29.03	138.3	61.5	65.0	0.4	0.5	44.0	48.3	41.9

Ht=plume height (kilometer above sampling height) calculated with the method of Carey and Sparks (1986) with the exception of (1) El Chichon A for which the height was calculated by Carey and Sigurdsson (1986) based on a modification of the method of Carey and Sparks (1986) in agreement with satellite observations (Schneider et al. 1999); (2) Pinatubo 1991 for which the maximum height is reported as determined by Holasek et al. (1996) based on the shadow and thermal methods (error of ±1.3). The method of Carey and Sparks (1986) for the same eruption resulted in an average value of 42 km (Rosi et al. 2001); and (3) Santa Maria 1902 for which the height was observed by a boat captain (Williams and Self 1983). The method of Carey and Sparks (1986) for the same eruption resulted in an average value of 34 km (Carey and Sparks 1986). *Ht**=plume height (in kilometer above sampling height) calculated from λ_{ML} vs Ht best fit (Fig. 4a). Associated error is 10 % (assuming that the mean error associated with the estimation of λ_{ML} is 20 %); *Ht***=plume height (in kilometer above sampling height) calculated from $\lambda_{Md\phi}$ vs Ht best fit (Fig. 4b). Associated error is 5 % (assuming that the mean error associated with the estimation of $\lambda_{Md\phi}$ is 10 %)

[a] Best fit obtained using weight $w=1/y$

References: Vesuvius 512 (Cioni et al. 2011); Averno (Di Vito et al. 2011); Boqueron (Garcia et al. 2012); Montaña 971 Blanca (Ablay et al. 1995); El Chichon (Carey and Sigurdsson 1986); Fogo A (Walker and Croasdale 1971); Fogo 1563 972 (Walker and Croasdale 1971); Agnano Monte Spina (de Vita et al. 1999); Cotopaxi Layer 3 and 5 (Biass and Bonadonna 2011; Tsunematsu 2012); Hatepe (Walker 1981a); Tarawera (Walker et al. 1984); Pululagua (Volentik et al. 2010); 974 Fontana Lapilli (Wehrmann et al. 2006; Costantini et al. 2009); Novarupta (Fierstein and Hildreth 1992); Quizapu 975 (Hildreth and Drake 1992); Santa Maria (Williams and Self 1983); Pinatubo 1991 (Holasek et al. 1996; Rosi et al. 2001); 976 Minoan (Bond and Sparks 1976); Taupo (Walker 1980); Waimihia (Walker 1981b)

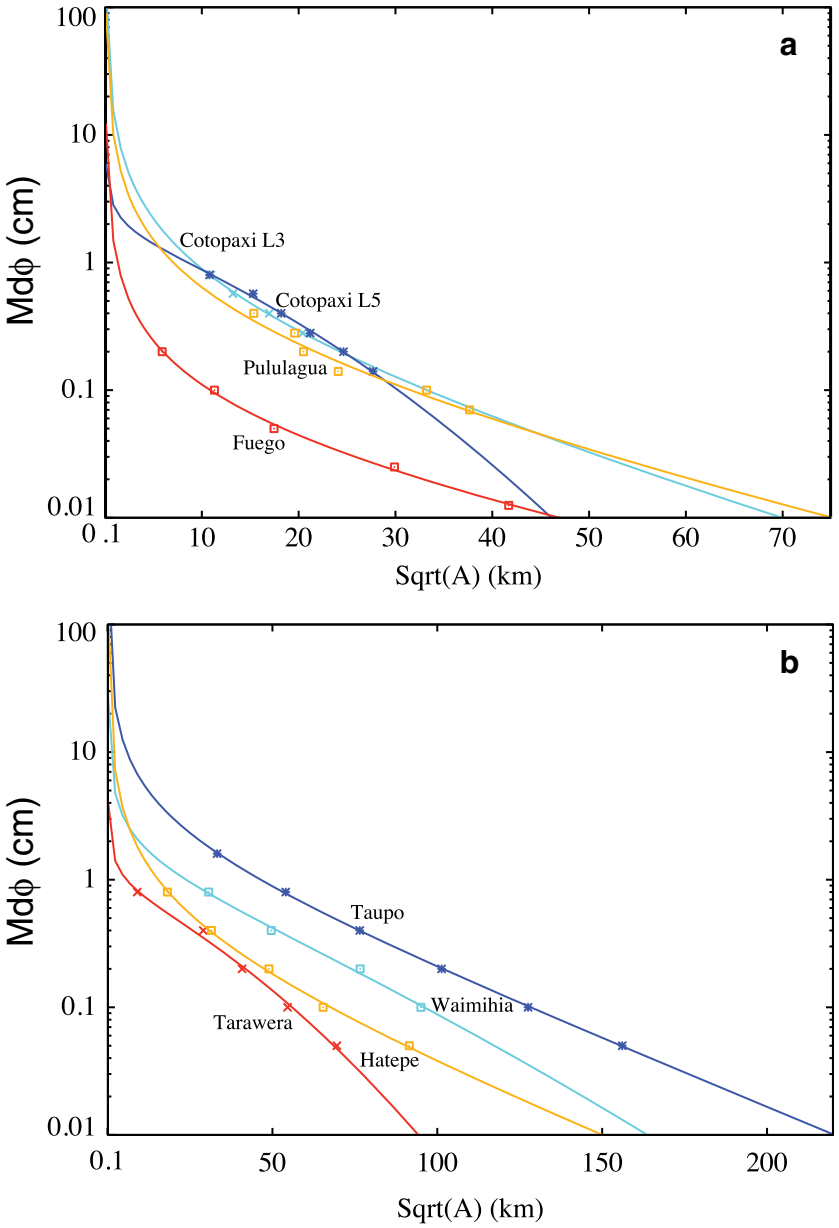

Fig. 2 Semilog plots of square root of contour area (in kilometers) versus Mdϕ (in centimeters) showing the Weibull best fit for various deposits on different length scales: **a** 70-km scale and **b** 200-km scale

Erupted volume and plume height

Weibull parameters have already been shown to describe important features of deposit thinning and to provide information on the eruption style and magnitude (Bonadonna and Costa 2012). In fact, λ_{th} represents the characteristic decay length scale of deposit thinning (typically expressed in kilometers), θ_{th} represents a thickness scale (typically expressed in centimeters), and n_{th} is a shape parameter (dimensionless). As a result, λ_{th} increases with eruption magnitude, with small and moderate eruptions (VEI ≤3) being characterized by values of λ_{th} <20 km (c.f. Figs DR3 of Bonadonna and Costa (2012)). Within each VEI class, θ_{th} increases with a decrease of λ_{th} (c.f. Figs DR2 of Bonadonna and Costa (2012)). Our dataset shows that λ_{th} correlates well with bulk erupted volume (Fig. 3) and, for all eruptions considered (Table 1), such a relationship gives the correct order of magnitude of the volume (typically within a factor of 4; dashed lines in Fig. 3). The associated empirical relation is:

$$\text{Volume}\left(m^3\right) = a_{th}\lambda_{th}^{bth} = 3{\cdot}10^6\lambda_{th}^{1.53} \quad (6)$$

with R^2=0.91 (30 data points with 2×10^6 m^3<volume<4×10^{10} m^3; Fig. 3).

Similarly, the Weibull parameters of the best fit for maximum clasts and Mdϕ also provide important insights on eruption style. In particular, both λ_{ML} and $\lambda_{Md\phi}$ correlate well with plume height (Fig. 4), and all eruptions considered are described within a factors 1.5 and 1.2, respectively (dashed line in Fig. 4a, b). Associated empirical relations are

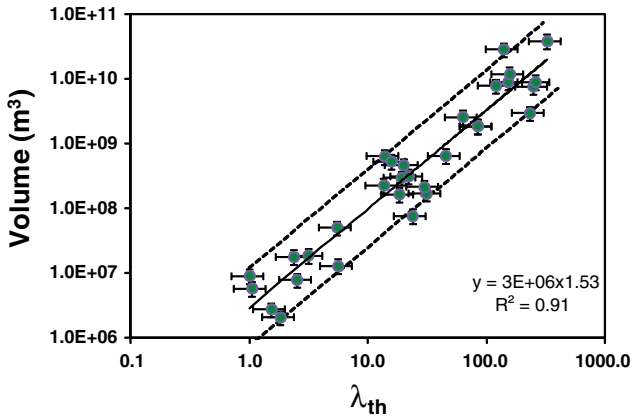

Fig. 3 Correlation between bulk erupted volume and λ_{th}. Typical mean errors of 25 % in the estimation of erupted volume with the Weibull best fit (from Table 1 of Bonadonna and Costa (2012)) and 30 % in the calculation of λ_{th} (from the typical average error in the fit determination) are also shown. Most estimations are within a factor 4 of the empirical equation (*dashed lines*)

$$\mathrm{Ht(km)} = a_{\mathrm{ML}}\lambda_{\mathrm{ML}}^{b\mathrm{ML}} = 5.01\lambda_{\mathrm{ML}}^{0.55} \quad (7)$$

with R^2=0.93 (30 data points with 7 km<Ht<50 km; Fig. 4a), for the Weibull parameter λ_{ML} derived from the relation between ML and square root of isopleth area, and

$$\mathrm{Ht(km)} = a_{\mathrm{Md}\phi}\lambda_{\mathrm{Md}\phi}^{b\mathrm{Md}\phi} = 4.98\lambda_{\mathrm{Md}\phi}^{0.51} \quad (8)$$

with R^2=0.85 (seven data points with 23 km<Ht<50 km; Fig. 4b), for the Weibull parameter $\lambda_{\mathrm{Md}\phi}$ obtained from the relation between Mdϕ and square root of the corresponding isograde area.

Plume height of all eruptions recalculated based on the new empirical relationships of λ_{ML} and $\lambda_{\mathrm{Md}\phi}$ are mostly within 25 and 15 % of previous estimates (Table 1). Results for the $\lambda_{\mathrm{Md}\phi}$ have to be considered carefully given the paucity of the cases analyzed.

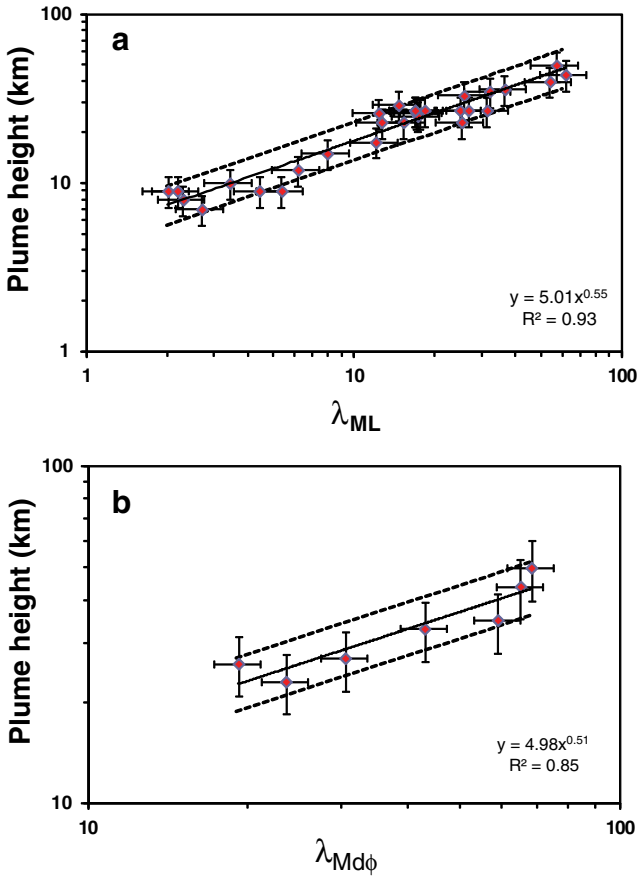

Fig. 4 Correlation of plume height versus **a** λ_{ML} and **b** $\lambda_{\mathrm{Md}\phi}$. *Error bars* of 20 % in the estimation of both Ht and λ_{ML}, and 10 % in the estimation of $\lambda_{\mathrm{Md}\phi}$ are also shown. *Dashed lines* indicate a maximum error of 25 % calculated for the parameters of Ht–λ_{ML} relationship (a_{ML} and b_{ML} in Eq. 7). A maximum error of 25 % is also assumed for the Ht–$\lambda_{\mathrm{Md}\phi}$ (Eq. 8) as only few data are available for fully determining the error on $a_{\mathrm{Md}\phi}$ and $b_{\mathrm{Md}\phi}$ in Eq. (8)

Eruption style

Several classification schemes have been proposed on the basis of eruption magnitude, plume height, and fragmentation index (e.g., Walker 1973, 1980; Self and Sparks 1978; Newhall and Self 1982; Pyle 1989, 2000; Cioni et al. 2008). In fact, there is no clear correlation between magnitude and plume height, and the fragmentation index is not only controlled by magma fragmentation but also by premature fallout of fine ash due to aggregation processes (e.g., Sparks et al. 1992; Pyle 2000). In addition, certain eruption styles, such as Vulcanian and Subplinian eruptions, might be characterized by similar plume heights and dispersal but very different source dynamics (e.g., pulsatory versus sustained plumes). Source dynamics are not always evident from tephra deposit features, and can only be constrained and characterized based on geophysical monitoring, which is not always available (e.g., infrasound, thermal imagery, seismic energy, deformation). As a result, the boundaries between different styles are often controversial. As an example, Pyle (1989) suggests a boundary between Strombolian/Subplinian, Subplinian/Plinian, and Plinian/Ultraplinian at 14 km (b_c=1 km), 29 km (b_c=3 km), and 45 km (b_c=8 km), respectively. Nonetheless, Sparks et al. (1992) found that the boundary between Subplinian/Plinian should be placed at a plume height of about 14 km based on analytical modeling. This is a value for which the dispersal index of Walker (1973) typically exceeds 500 km^2. Cioni et al. (2008) introduced a classification for activity at Vesuvius that includes: ash emission (<5 km; VEI2-3), violent Strombolian (5–10 km; VEI2-3), Subplinian II (10–15 km; VEI3), Subplinian I (15–20 km; VEI4), and Plinian (>20 km; VEI5). Finally, even though it is well established that plume height of past eruptions can only be constrained with a typical error of 20 % (e.g., Carey and Sigurdsson 1989; Oddsson et al. 2012), none of these

classification schemes consider uncertainty explicitly, which makes eruption classification even more problematic.

Here, we present a simplified eruption classification based on plume height and intensity (related to the intensity and dispersal power parameters of Walker (1980)) assuming a typical error of 20 % (Fig. 5). First, we consider an ideal Plinian eruption being characterized by a plume height of 30 km, similar to the Gray Pumice phase of the 79 AD eruption described by Plinius the Younger, as also suggested by Sparks et al. (1997) as a reference eruption. This choice is based on the estimation made by Carey and Sigurdsson (1987) using the model of Carey and Sparks (1986), and by Pfeiffer et al. (2005) by inversion of the tephra deposits. For the Gray Phase, Carey and Sigurdsson (1987) estimated the column increased to a maximum of 32 km and then decreased to about 27 km, whereas Pfeiffer et al. (2005) estimated a column between 27 and 30 km. Second, we define the plume height of an ideal Subplinian eruption by decreasing the mass eruption rate (MER) 1 order of magnitude with respect to the ideal Plinian eruption. Using Mastin et al. (2009) empirical scaling, i.e., $\mathrm{MER}(H)\approx aH^{4.15}$, we have that the MER ratio relative to two column of height H_1 and H_2 is

$$\frac{\mathrm{MER}(H_1)}{\mathrm{MER}(H_2)}\approx\left(\frac{H_1}{H_2}\right)^{4.15} \tag{9}$$

This implies that the ideal Subplinian eruption has a column height of ~17 km, based on the scaling of the ideal Plinian column (30 km) by a factor 0.575 (i.e., $0.575^{4.15}\cong 0.1$). Similarly, moderate–small explosive eruptions are associated with a plume height of 10 km (i.e., 17 km multiplied by 0.575). The boundaries between the different eruption classes are chosen at the intermediate points. Hence, the boundary between Plinian and Subplinian eruptions is at 24 km (the midpoint between 30 and 17 km approximated to 1 km), and the boundary between small–moderate explosive eruptions and Subplinian eruptions is at 14 km (the midpoint between 17 and 10 km). Eruptions classified as Subplinian using this method are the eruptions that typically reach the stratosphere and include Subplinian I of Cioni et al. (2008). Given that below ~10 km (i.e., tropospheric eruptions) the MER does not depend only on plume height but can be strongly affected by wind conditions (Degruyter and Bonadonna 2012; Folch et al. 2012), we do not subdivide further the category of small–moderate explosive eruptions, which include Vulcanian, Strombolian, Hawaiian, violent Strombolian, and continuous ash emissions and Subplinian II of Cioni et al. (2008). Further characterization of moderate–small explosive eruptions should be based on detailed geophysical information and on componentry and textural analysis when available, as typically they cannot be discriminated only from plume height and tephra dispersal. Finally, if we increase the MER of 1 order of magnitude with respect to Plinian eruptions to define the Ultraplinian eruptions, we obtain a nominal column of 52 km. Although this value may be too high to be realistic, considering the midpoint between 30 and 52 km, the transition between Plinian and Ultraplinian is set at 41 km. When this classification scheme is used, a typical minimum 20 % error in the calculation of plume height and a factor 4 spread in the calculation of MER should be considered (error bars in Fig. 5; Carey and Sigurdsson 1989; Mastin et al. 2009). Figure 5 also shows

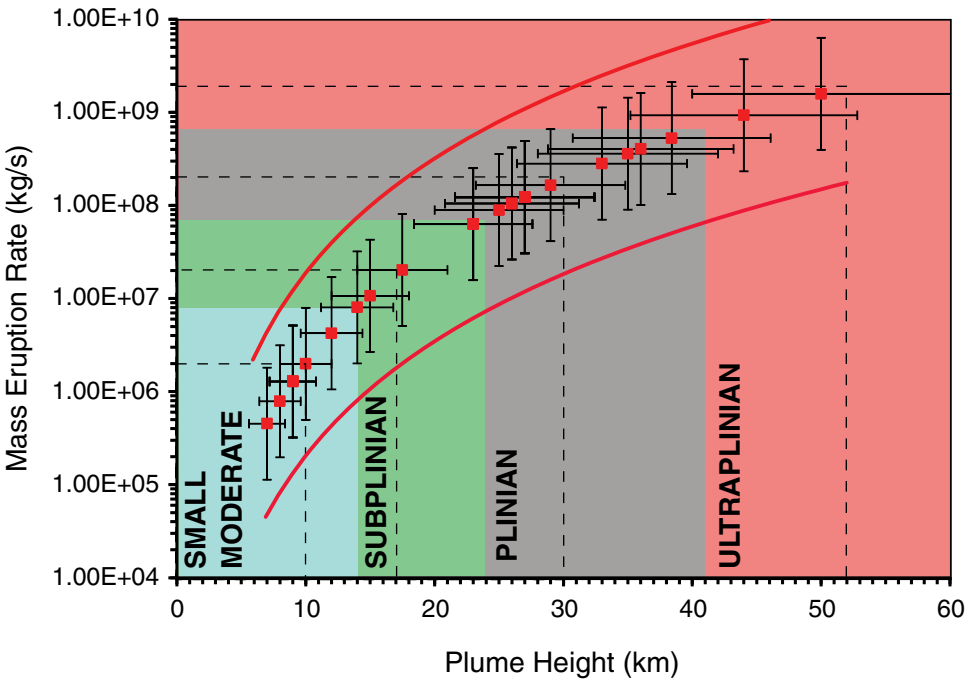

Fig. 5 Classification plot for tephra deposits based on the determination of plume height and MER estimated in accord to the parameterization Mastin et al. (2009). Eruption cases reported in Table 1 and associated error of 20 % in the calculation of plume height is also shown. *Vertical error bars* show a typical spread of a factor 4 for MER values as reported by Mastin et al. (2009). *Red solid lines* indicate a the field of possible Ht-MER values based on a factor 10 deviation from the Mastin et al. (2009) relationship (Degruyter and Bonadonna 2012)

the typical values of Ht-MER as predicted by the relationship of Mastin et al. (2009) based on a discrepancy of a factor 10 from a 1D model as suggested by Degruyter and Bonadonna (2012; solid red lines).

New eruption classification schemes

Considering the boundaries between eruption styles as defined in Fig. 5, explosive volcanic eruptions can be classified based on plume height by plotting λ_{th} versus $\lambda_{ML}/\lambda_{th}$ (Fig. 6). All eruptions in Table 1 agree within a 20 % error with height boundaries identified by the combination of λ_{th} and $\lambda_{ML}/\lambda_{th}$. This implies that eruptions with plume height close to the identified boundaries could be equally classified by two adjacent styles. As an example, the Minoan eruption (#28 in Table 1 and Fig. 6) plots in the lower 20 % boundary of Plinian–Ultraplinian eruptions, with an estimated plume height of 36 km. Both Taupo (#29) and Waimihia (#30) plot within the upper 20 % boundary of Plinian–Ultraplinian eruptions even though the associated plume height was estimated at about 50 and 44 km, respectively. We can define these eruptions as transitional Plinian to Ultraplinian. In contrast, Hatepe (#17) can be univoquely classified as Plinian as it plots outside the 20 % boundary between Plinian and Ultraplinian. Similarly, all Averno eruptions and Boqueron can be classified as small–moderate explosive eruptions as they plot below the 20 % boundary of 14 km (eruption numbers 2–7 in Table 1 and Fig. 6). Considering the uncertainty associated with the determination of both the Weibull parameters and plume height, even recent well-studied eruptions could plot in the transitional fields. As an example, the maximum plume height associated with the Pinatubo 1991 eruption was estimated to be 40±1.3 km by both shadow and thermal method (eruption #27 in Table 1 and Fig. 6; Holasek et al. 1996), and corresponding Weibull-derived Ht, λ_{th}, and $\lambda_{ML}/\lambda_{th}$ are similar to those of Ultraplinian eruptions (i.e., Ht=44.8 km; λ_{th}=229.6; $\lambda_{ML}/\lambda_{th}$=0.2). In fact, according to our scheme, Pinatubo 1991 plots within the upper 20 % boundary of Plinian–Ultraplinian. Considering a 20 % uncertainty, Pinatubo 1991 could be classified as transitional Plinian–Ultraplinian even based on the average height determined with the method of Carey and Sparks (1986; i.e., Ht=42 km; Rosi et al. 2001).

Similarly, volcanic eruptions can be classified based on plume height by plotting λ_{th} versus $\lambda_{Md\phi}/\lambda_{th}$ (Fig. 7). However, given the scarcity of data for the determination of the relation between $\lambda_{Md\phi}$ and Ht (Fig. 4b), this second classification scheme needs to be considered as preliminary. In particular, the fields of the small–moderate and Subplinian eruptions of Fig. 7 are not supported by observations as plume height values of our dataset only range between 23 and 50 km (see Eq. 8).

Nonetheless, with this classification scheme again both Taupo and Waimihia (red squares) plot as transitional Plinian to Ultraplinian, whereas Hatepe (λ_{th}=44.8, λ_{ML}=32.0, $\lambda_{MD\phi}$=58.9) plots as transitional Plinian to Ultraplinian, in contrast with the λ_{th} and vs. $\lambda_{ML}/\lambda_{th}$ classification that defined it as uniquely Plinian (Fig. 6). Tarawera eruption is classified as Plinian, and Pululagua and both Cotopaxi layers 3 and 5 plot in the range of transitional Suplinian to Plinian.

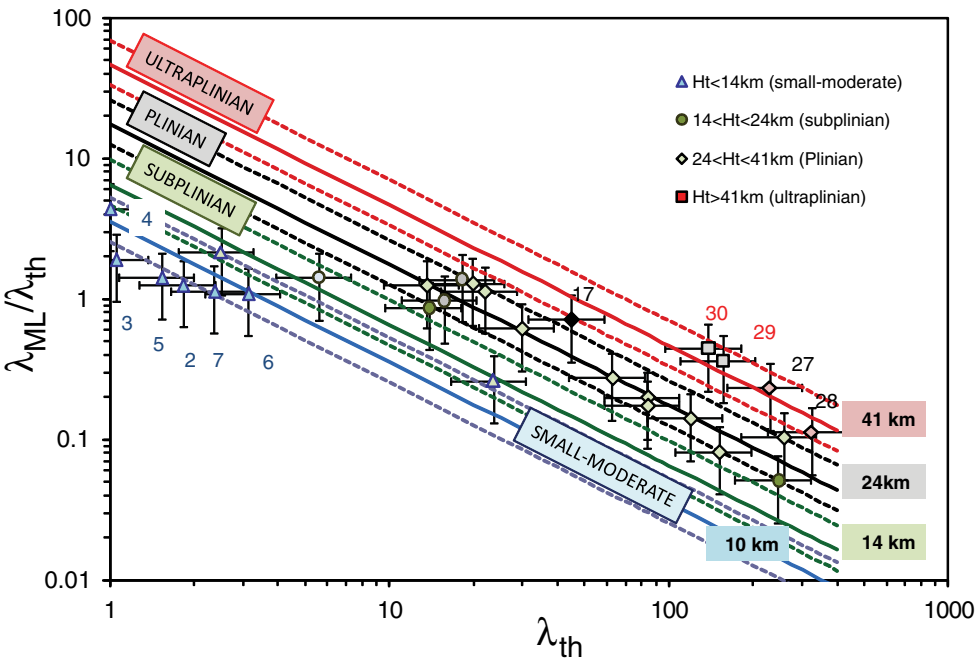

Fig. 6 New classification scheme for tephra deposit based on the correlation of λ_{th} versus $\lambda_{ML}/\lambda_{th}$. *Red*, *black*, and *green solid lines* represent theoretical lines for Ht of 41, 24, and 14 km, respectively, based on the correlation of Eq. 7. Ht of 10 km (*blue solid line*) is also shown for reference. Associated 20 % error is indicated with *dashed lines of the same color*. Data from selected eruptions (Table 1) are also shown with different symbols depending on their plume height. *Error bars* of 30 and 50 % are also shown for the estimation of λ_{th} and $\lambda_{ML}/\lambda_{th}$, respectively. *Numbers* indicate key eruptions discussed in the text and reported in Table 1

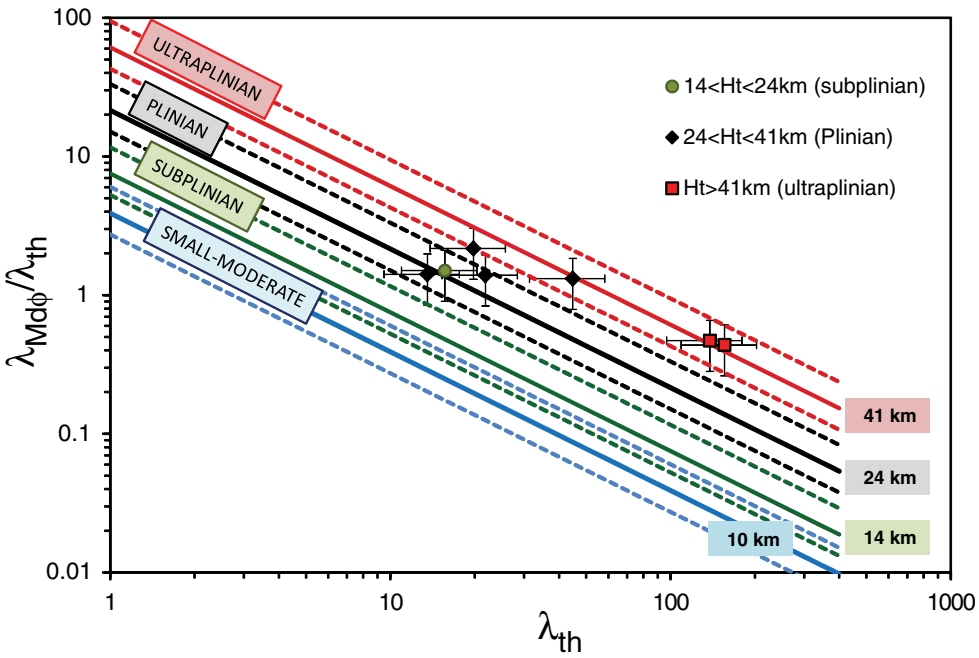

Fig. 7 New classification scheme for tephra deposit based on the correlation of λ_{th} versus $\lambda_{Md\phi}/\lambda_{th}$. *Red*, *black*, and *green solid lines* represent theoretical lines for Ht of 41, 24, and 14, respectively, based on the correlation of Eq. 8. Ht of 10 km (*blue solid line*) is also shown for reference. Associated 20 % error is indicated with *dashed lines* of same color. Data from selected eruptions (Table 1) are also shown with different symbols depending on their plume height. *Error bars* of 30 and 40 % are also shown for the estimation of λ_{th} and $\lambda_{Md\phi}/\lambda_{th}$, respectively

Discussion

Tephra deposits retain important information on the height and dynamics of eruptive columns and are typically used to classify the associated eruptive style. Nonetheless, a standard strategy for the estimation of erupted volume and eruption style still does not exist. The Weibull function has been introduced for the calculation of both erupted volume (Bonadonna and Costa 2012) and plume height and for the classification of explosive volcanic eruptions in order to address shortcomings of previous strategies (e.g., choice of multiple segments for the exponential method and volume underestimation in case of missing segments; choice of extremes of integration for the power law method; lack of universal boundaries between different eruptive styles for eruption classification). Nevertheless, all models and strategies have advantages and disadvantages that need to be critically considered in order to best interpret the associated results. Main issues associated with best fitting methods, with the determination of eruptive parameters and with eruption classification, are discussed below.

Best fitting method: suggestions and limitations

The evaluation of the Weibull parameters for the estimation of volume (e.g., from isopach contours) and column height (e.g., from maximum lithic or Mdϕ isolines) can be implemented by using various free software packages (e.g., Grace, R). However, we have also compiled a Microsoft Excel® template. For all cases analyzed in this study (Table 1), we used the nonlinear curve fitting algorithm of the free software Grace minimizing the relative square error. Although algorithms like the Grace nonlinear curve fitting algorithm are quite stable and more general than the Microsoft Excel® template, there could be problems with fitting cases that have few data, missing regions (e.g., proximal or distal), or in general low-quality data. In these cases, the expertise of the user becomes very important. Often these cases are characterized by parameter values that lay at the border of the chosen ranges. First, it is recommended to estimate roughly the VEI of the eruption (here, we use VEI for a sake of simplicity as not all deposit densities are well known; alternatively, eruption magnitude may be utilized instead of VEI), using exponential and/or power law integrations. Second, it is suggested to restrict the range of values for ϕ_{th} and λ_{th} and λ_{ML}, depending on the VEI using the ranges presented in Table 2. The range for n_{th} can be set as $0.2 \leq n_{th} \leq 2$; the range for θ_{ML} can be set as $1 \leq \theta_{ML} \leq 20$ cm; and the range for n_{ML} can be set as $0.5 \leq n_{ML} \leq 2$. Commonly, the relative square error is minimized corresponding to the

Table 2 Ranges of Weibull parameters recommended for the calculation of volume and plume height according to individual VEI (see text for details). The suggested range for n_{th} is $0.2 \leq n_{th} \leq 2$; whereas for n_{ML} is $0.5 \leq n_{ML} \leq 2$. The range for θ_{ML} can be set as $1 \leq \theta_{ML} \leq 20$ cm

VEI	θ_{th} (cm)	λ_{th} (km)	λ_{ML} (km)
1	0.1–10.0	0.2–20	1.0–10.0
2	5.0–500.0	0.5–5.0	1.0–10.0
3	3.0–300.0	1.0–20.0	1.0–10.0
4	2.0–200.0	5.0–100.0	5.0–50.0
5	1.0–100.0	20.0–400.0	10.0–100
6	1.0–100.0	50.0–1,000.0	10.0–100

Table 3 Sensitivity tests carried out for the eruptions of Novarupta C (four isopleth contours), Vesuvius 512 U5 (four isopach contours) and Cotopaxi layer 3 (six isopach contours) for the effect of a potential underestimation of the area of the last contour on the calculation of plume height (from Eq. (7)) and erupted volume (from Eq. (3))

Novarupta C	θ_{ML} (cm)	λ_{ML} (km)	n_{ML}	Ht (km)
$w^i=1/T_i^2$	10.70	17.23	1.82	24.0
$w^i=1/T_i$	10.65	16.40	1.59	23.3
Deletion of most distal point	8.80	17.77	1.23	24.4
Vesuvius 512 U5	θ_{th} (cm)	λ_{th} (km)	n_{th}	Volume (km^3)
$w^i=1/T_i^2$	42.07	5.57	1.92	0.01
$w^i=1/T_i$	38.30	5.70	1.77	0.01
Deletion of most distal point	21.91	8.01	1.41	0.02
Cotopaxi layer 3	θ_{th} (cm)	λ_{th} (km)	n_{th}	Volume (km^3)
$w^i=1/T_i^2$	192.03	15.66	1.74	0.54
$w^i=1/T_i$	194.11	15.61	1.75	0.54
Deletion of most distal point	199.64	15.23	1.58	0.59

use of the weight $w^i=1/T_i^2$ (Bonadonna and Costa 2012). However, depending on the quality of data, other weights can be used. Ideally, the error associated with deposit thickness, maximum clast or median grain size should be estimated and uncertainties associated with isopach or isopleth contours should also be assessed based on the number of outcrops available, so that the actual errors could be used as weight in the best fit minimization. Special attention should be given to the uncertainty associated with the calculation of the area of the most distal contour. In fact, it is important to note how often the most distal contour of isopach, isopleth, and Mdϕ maps forces a convex shape to the Weibull trend as opposed to a more common concave shape. This is likely due to the fact that the area of the most distal contour cannot be well constrained, due to the paucity of distal outcrops, and corresponding values are often underestimated. As a result, it is very important to critically assess the uncertainty associated with the most distal contour point. If this point is considered unreliable, then more weight should be given to the proximal and medial points. Alternatively, such a point can be eliminated from the calculation (the best guess should lay between the two estimations). A test carried out on the case of Novarupta C (Figs. 1c and 8a; Table 3) shows how λ_{ML} is not significantly affected by the strategy used to treat the last contour (i.e., $w^i=1/T_i^2$ strategy, $w^i=1/T_i$ strategy and the elimination of the last contour point) and, therefore, the calculation of plume height and eruption classification should not be significantly affected (Figs. 4 and 6). However, the strategy used to treat the last contour might significantly affect the calculation of erupted volume in case of a limited dataset (i.e., where only few outcrops are available). In fact, the point associated with the last contour mainly influences the shape parameters that affect the volume calculation (Eq. 3) and not the estimation of plume height (Eq. 7; Table 3). Two examples were selected to show the effect of the underestimation of the area of the last isopach contour on the volume calculation in case of a small dataset (i.e., Vesuvius 512 U5; Table 3; Fig. 8b) and a larger dataset (Cotopaxi layer 3; Table 3; Fig. 8c). Clearly, the last point has more weight in the case of the Vesuvius dataset, with the elimination of the most distal contour point resulting in a volume 46 % larger than the estimation based on the $w^i=1/T_i^2$ weight (Table 3). In contrast, the elimination of the last point in the Cotopaxi example only results in a volume 8 % larger than the estimation based on the $w^i=1/T_i^2$ weight (Table 3).

The use of maximum clast and median grain size for the calculation of plume height and eruption classification

The decrease in the size of maximum clasts with distance from vent was already introduced by Carey and Sparks (1986), Wilson and Walker (1987), and Pyle (1989) for the calculation of plume height and, in combination with thickness data, for the classification of explosive eruptions (Pyle 1989). Pyle (1989) showed how relations of ideal isopleth areas and maximum clast size identify single slopes associated with specific plume heights, which are almost independent of clast density. As a result, both pumice and lithic clasts could theoretically be used to calculate plume height and classify explosive eruptions. Nonetheless, the use of the largest lithic clasts is preferred to the largest pumice clasts as lithic fragments are less breakable with impact with the ground and, therefore, the associated isopleth maps best represent the original clast dispersal from volcanic plumes (Walker 1980; Bonadonna et al. 2013). However, Bonadonna et al. (2013) have discussed the complexity of the determination of the maximum clasts and the lack of a standardized strategy, which often result in a large discrepancy of outcomes. In this context, the use of Mdϕ could lead to a more stable and comparable determination of plume height and eruption classification. Even though Pyle (1989) suggests that b_c associated with both maximum and median grain size are similar, Sparks et al.

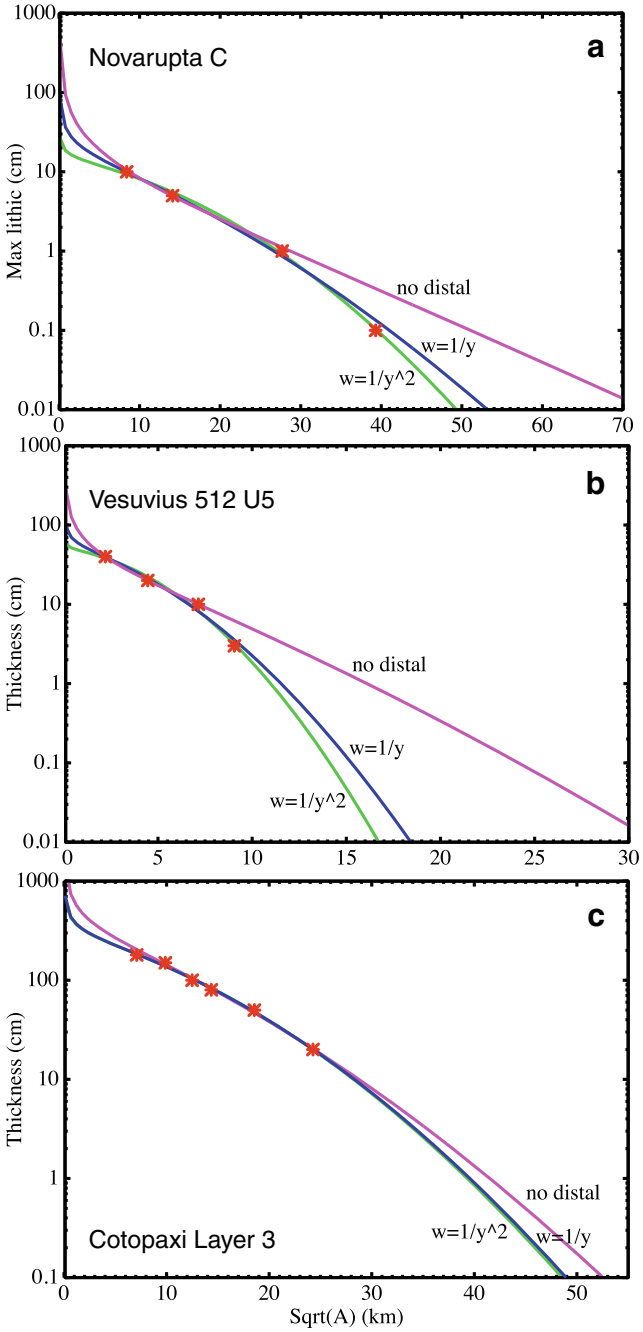

Fig. 8 Sensitivity test for the study of the influence of the potential underestimation of the area of the last contour on the general trend for: **a** Novarupta C, **b** Vesuvius 512 U5, **c** Cotopaxi layer 3

(1992) found that b_c associated with maximum clasts are commonly smaller than b_c associated with median grain size. We also found that λ_{ML} is typically smaller than $\lambda_{Md\phi}$ (Table 1). However, as showed by relationships (7) and (8), the exponents characterizing the relationships between Ht and λ_{ML} and Ht and $\lambda_{Md\phi}$ are very similar (~0.5). The main shortcomings for Mdϕ are: (1) calculation of Mdϕ of bimodal distributions, (2) premature fallout of fine ash, (3) density difference between juvenile and lithic components, and (4) lack of a large number of Mdϕ maps in the literature necessary for a wide application and validation of such a method.

Premature fallout of fine ash mainly due to particle aggregation has been discussed by Pyle (1989) and Sparks et al. (1992) that highlight the complexity of defining a fragmentation index based on deposit grain size, e.g., F of Walker (1973). In fact, variation of grain size with distance from vent not only will depend on magma fragmentation but also on dispersal and deposition conditions. Sparks et al. (1992) suggest that the parameters b_t and b_c of Pyle (1989) might also be affected by particle aggregation. Nevertheless, given that premature fallout of fine ash often results in bimodality, with the coarser mode representing the population of particles that did not aggregate, we suggest using the mode of the coarse population instead of Mdϕ on the entire distribution. Deposits for which aggregation does not result in bimodal grain size distribution (e.g., 2010 eruption of Eyjafjallajökull volcano, Iceland; Bonadonna et al. 2011) should be interpreted as the populations of particles fallen individually and fallen as aggregates roughly overlap, in which case Mdϕ can be considered as representative of the fallout of individual particles (unless all particles aggregated).

In some cases, bimodality can also be related to density differences between juvenile and lithic clasts (e.g., Cioni and Sulpizio 1998; Sulpizio et al. 2010). We consider that such differences are only relevant for the coarse fractions, as the density of particles smaller than 250 μm tend to converge to the lithic density (e.g., Eychenne and Le Pennec 2012). However, grain size distributions of lithic-rich deposits should be carefully analyzed and interpreted. A possible alternative would be to consider terminal velocity isograde maps instead of grain size isograde maps, but these are even fewer than the Mdϕ maps and could be associated with larger uncertainties related to the choice of the model used to determine terminal velocity and assumptions on particles shape (e.g., Walker and Croasdale 1971; Walker 1980; Walker et al. 1984). Considering the difficulties of determining the maximum clasts and the promising correlations shown by Fig. 4b, we consider the use of Mdϕ values for the calculation of plume height and classification of explosive eruptions as a viable alternative to the use of ML and MP. However, more Mdϕ maps should be compiled and analyzed to investigate the applicability and limitations of such a method. Finally, another parameter that could represent an alternative to both ML and Mdϕ data is the 50th percentile of a 20-clast sample as suggested by Bonadonna et al. (2013). Again, more data are necessary to build more solid correlations with plume height.

Calculation of erupted volume and plume height

We have shown how Weibull parameters correlate well with both erupted volume (Fig. 3) and plume height (Fig. 4). In particular, estimations of volume based on Eq. (6) can give

the proper order of magnitude with typical uncertainties delimited by a factor 4 and 0.25, respectively. Nonetheless, the calculation of erupted volume is recommended by integration of the Weibull function as described by Bonadonna and Costa (2012; i.e., Eq. 3). Plume height can be well constrained (with a maximum error of 25 % and a mean error of about 10 %) based only on the Weibull parameter λ_{ML} and the empirical Eq. (7) (in particular our dataset consists of plume heights ranging between 7 and 50 km). The use of $\lambda_{Md\phi}$ for the calculation of plume height is also promising (Fig. 4b and Eq. 8), but more case studies are needed to better constrain the associated empirical equation. Another important issue associated with the determination of plume height from grain size trends is the actual interpretation of the results. In fact, the height associated with the method of both Carey and Sparks (1986) and Pyle (1989) and with Eq. (7) represents the maximum height as it is typically derived from the distribution of the largest clasts around the volcano. In contrast, the height derived based on Mdϕ should be considered as an average height, as the median grain size represents an "average" picture of the eruptive conditions instead of the extreme dispersive capability of the eruption that can be derived from the distribution of the largest clasts (e.g., Walker 1980). It is also important to consider that the height represents the height above the sampling level, which is typically intermediate between the height above sea level and the height above the vent. Other empirical strategies of determining plume height from tephra deposits include the method of Sulpizio (2005) based on the proximal thickness decay and the methods of Bonadonna et al. (1998) and Bonadonna and Phillips (2003) based on the position of breaks-in-slope in the thinning trend. Multiple methods should be considered in order to better assess uncertainty.

Eruption classification

Hazard assessment and physical characterization of explosive volcanoes build on the determination of eruptive parameters discussed above and on the classification of eruption style of past and expected future eruptions. However, eruptions are not always classified based on the same criteria and often dedicated schemes are required for individual volcanoes in order to capture local trends and specific eruptive patterns (e.g., Arrighi et al. 2001; Branca and Del Carlo 2005; Andronico et al. 2008a; Cioni et al. 2008; Cole et al. 2013; Rosi et al. 2013). Nonetheless, a broader classification scheme is needed in order to make global comparisons, to better understand general trends of explosive volcanoes and to better identify the key processes that differentiate eruptive styles. The pioneering classification scheme introduced by Walker (1973) based on the D (area over which a deposit thins to 0.01 of its T_{max}) and F (percentage of ash finer than 1 mm at the point where the isopach corresponding to 1/10 of T_{max} crosses the dispersal axis) helped, for the first time, to describe and distinguish explosive eruptions in a quantitative way. Along the base of the diagram (x-axis; i.e., increasing eruption intensity and dispersal power) we find eruptions characterized by an increase in magma viscosity and/or gas content: Hawaiian, normal Strombolian, Subplinian, and Plinian. Then, two distinct relationships developing along the y-axis of the diagram (i.e., decreasing grain size distribution) are identified for basaltic and silicic eruptions as a consequence of an increase of the explosion violence that results in a higher degree of fragmentation: violent Strombolian to Surtseyan eruptions for the basaltic trend and Vulcanian/Vesuvian to silicic equivalent of Surtseyan for the more silicic trend. A third trend was also recognized going towards small dispersal and high fragmentation for weak explosions (probably equivalent to continuous ash emissions of Cioni et al. (2008)). The diagram of Walker (1973) was slightly modified by Walker (1980) and Self and Sparks (1978) and redrawn by Wright et al. (1980)) to introduce Ultraplinian (characterized by a wider dispersal; i.e., D>50,000 km^2) and Phreatoplinian (i.e., silicic equivalent of Surtseyan) eruptions, respectively. These different styles can also be identified based on their capacity to generate sheet- (Subplinian to Ultraplinian) or cone-like (Hawaiian and Strombolian) tephra deposits.

The idea of Walker (1973, 1980) to classify explosive eruptions based on the quantitative description of tephra deposits as opposed to sporadic visual observations of eruptions contributed to an amazing progress in volcanology and to the consolidation of modern physical volcanology. Deposits have been studied based on these principles until the 1990s (e.g., Self et al. 1974; Bond and Sparks 1976; Booth et al. 1978; Walker 1981a; Walker et al. 1984). Shortcomings of this scheme include: (1) the difficulty of determining D, F, and T_{max} (e.g., Fisher and Schmincke 1984); (2) the actual meaning of the fragmentation index discussed in the previous section (e.g., Pyle 1989); (3) the poor constraint on the Hawaiian field (Houghton and Gonnermann 2008); (4) the absence of volcanic products other than tephra deposits (e.g., ratio of lava to tephra volume important for the classification of more mafic eruptions (Pioli et al. 2009)); and (5) the absence of hybrid and multistyle eruptions that might cross different categories (e.g., Sparks et al. 1997). Pyle (1989) introduced a new classification scheme based on the b_t and the half-distance ratio (b_c/b_t) that does not need complex grain size analysis and it is mainly based on plume height. Ultraplinian, Plinian, Subplinian, Strombolian, and Surtseyan eruptions are identified, even though the diagram works best for Plinian, Subplinian, and Ultraplinian. The main shortcomings associated with the classification scheme of Pyle (1989) include the ambiguity associated with the choice of b_t and b_c/b_t parameters to use in case of multiple segments for both isopach and isopleth plots and

the boundaries between different eruptive styles, as discussed and questioned by Sparks et al. (1992).

Our new simplified classification scheme has the same advantage of that of Pyle (1989), in that it is based on Weibull parameters of easier determination with respect to D, F, and T_{max} of Walker (1973, 1980). In addition, Weibull parameters are unique for all deposits and, therefore, there is no ambiguity on the choice of λ_{th} and λ_{ML}. Finally, our choice of boundaries between different eruptive styles is based on a simple quantitative scaling of intensity (i.e., MER) with respect to an ideal Plinian eruption (taken as the Gray Pumice phase of the 79 AD eruption described by Plinius the Younger that was characterized by a 30-km-high plume). Given the simplified approach only based on plume height and intensity, we could only identify Ultraplinian, Plinian, Subplinian (having typical eruption columns reaching the stratosphere), and small–moderate explosive eruptions (typically confined to the troposphere). In fact, we did not attempt to also describe more complex eruptions, such as Surtseyan and Phreatoplinian, which would require information on the fragmentation mechanisms, that, as also highlighted by Pyle (1989) and Sparks et al. (1992), would be difficult to obtain based only on grain size variations with distance from vent. In addition, we did not further subdivide small–moderate explosive, as plume height of tropospheric eruptions is strongly affected by wind speed (e.g., Degruyter and Bonadonna 2012; Folch et al. 2012).

Small–moderate explosive eruptions include Vulcanian, Strombolian, Hawaiian, Violent Strombolian, and continuous ash emissions and Subplinian II of Cioni et al. (2008). Clearly, these eruptions (typically associated with a VEI 2–3) need to be distinguished based on source dynamics, as highlighted by geophysical monitoring (e.g., pulsating versus sustained activity, seismic energy, and ground deformation) and on a detailed analysis of the associated pyroclastic deposits (e.g., general grain size of the deposit, massive versus graded deposits, textural features, componentry, density of products, and porosity; (e.g., Cashman 2004; Mueller et al. 2011; Rust and Cashman 2011)). As an example, Cioni et al. (2008) distinguishes between Subplinian I and II based on the presence of pyroclastic density currents. As a consequence, our new classification scheme is appropriate for large eruptions and for global comparisons, similarly to what already discussed by Cioni et al. (2008) in relation to the use of the VEI scale. Detailed local studies and hazard assessments of volcanoes characterized mainly by small–moderate explosive eruptions would then require dedicated classification schemes (e.g., recent activity of Etna volcano, Italy; e.g., Scollo et al. (2007), Andronico et al. (2008a, b), and Norini et al. (2009)).

A comprehensive and widely applicable classification scheme should eventually merge intensity, deposit features and geophysical observations in order to capture the whole spectrum of eruptive style from weak explosions to Ultraplinian eruptions (e.g., Gurioli et al. (2008, 2013)). In fact, weak explosions are often not even capable of producing extensive tephra deposits and are, therefore, better characterized on the basis of geophysical observations (Marchetti et al. 2009; Patrick et al. 2007; Ripepe et al. 1993). In contrast, large Plinian and Ultraplinian eruptions are so infrequent and destructive that they are more easily studied based on deposit features than on geophysical monitoring (e.g., Taupo (Walker 1980), Tambora (Self et al. 1984), Minoan (Pyle 1990), and Pinatubo 1991 (Newhall and Punongbayan 1996)).

Regardless of the classification scheme considered, it is very important to quantitatively characterize the uncertainty associated with the parameters used. The description of such uncertainty is crucial to any hazard assessment and evaluation of future eruptions at any given volcano. Finally, it is important to notice how there is, in fact, a continuum between various eruptive styles and how many eruptions are characterized by multiple styles, e.g., they can start phreatomagmatic and continue as dry events (e.g., Ruapehu 1996; Eyjafjallajökull 2010 (Bonadonna et al. 2005; Gudmundsson et al. 2012)) or start as magmatic eruptions and have a final phreatomagmatic event, as for most of Vesuvian eruptions (e.g., Carey and Sigurdsson (1987); Bertagnini et al. (1991)). Classification schemes might not be able to describe such complexity and often these variations in style are not even very well captured in the stratigraphic record and individual units cannot be distinguished. As a result, associated thinning and grain size variations should be considered as an average of the various eruptive styles or as representative of the major style.

Conclusions

The Weibull function has been shown to accurately describe variation in both thickness and grain size of tephra deposits with distance from vent. As a result, Weibull parameters can be used to determine eruptive features (i.e., erupted volume and plume height) and classify explosive volcanic eruptions. In particular:

1. Erupted volume can be determined as described by Bonadonna and Costa (2012; Eq. 3).
2. Plume height can be determined with a typical error of 10–15 % and a maximum error of 25 %, based on an empirical equation relating λ_{ML} and plume height (Eq. 7). Preliminary results show that also $\lambda_{Md\phi}$ well correlates with plume height (Eq. 8).
3. The Weibull function well describes the natural thinning and grainisze variations of tephra deposits. However, a different best-fitting strategy (e.g., weights $w^i = 1/T_i^2$, the

$w^i = 1/T_i$ or, even better, the actual individual errors) should be used based on the uncertainty associated with each thickness/grain size contour versus square root of area set of value. Such uncertainty should be quantified when compiling isopach, isopleth, and Mdϕ maps.

4. Boundaries between different eruptive styles were determined based on a simple intensity scaling and result in 41, 24, and 14 km for Ultraplinian/Plinian, Plinian/Subplinian and Subplinian/small–moderate explosive eruptions, respectively.
5. Ultraplinian, Plinian, Subplinian, and small–moderate explosive eruptions can be classified based on a plot of λ_{th} versus $\lambda_{ML}/\lambda_{th}$. Small–moderate explosive eruptions (e.g., Hawaiian, normal Strombolian, violent Strombolian, Vulcanian eruptions, and continuous ash emissions) cannot be further subdivided based only on plume height and intensity, and require detailed geophysical and/or field studies to be classified.
6. Our new classification scheme can be best applied for the classification of large explosive eruptions and for global comparisons, whereas dedicated classification schemes based on local eruptive patterns should be developed for hazard assessment of volcanoes characterized mainly by small–moderate explosive eruptions.
7. An effort should be made to merge eruption intensity, deposit features, and geophysical information in order to generate a comprehensive classification scheme that can cover the whole range from weak explosions to Ultraplinian eruptions.
8. Any classification scheme should account for the uncertainty associated with the determination of both plume height and classification parameters (e.g., D and F of Walker (1973), b_t and b_c of Pyle (1989) and Weibull parameters). Accounting for such an uncertainty highlights how most eruptions can be, in fact, classified as transitional between adjacent eruptive styles (e.g., Figs. 6 and 7).

Acknowledgments The authors are grateful to L. Pioli and R. Cioni for discussion of an earlier version of the manuscript. A. Costa was funded by the Italian Dipartimento della Protezione Civile in the ambit of the Project "V1", agreement INGV-DPC 2012–2013. R. Sulpizio, an anonymous reviewer and the Associate Editor J. Gardner are thanked for constructive comments that have improved the manuscript.

Appendix 1

According to the model of Bursik et al. (1992), based on the assumptions that i) the atmosphere in which the eruptive plume develops is continuously stratified; ii) the wind field at the spreading current level is constant; iii) the volume flux in the spreading current is constant with distance (i.e., there is no air entrainment within the spreading current); iv) particles are vertically well mixed by turbulence in the spreading current; v) the concentration of particles in the cross-wind direction of the spreading current has a Gaussian distribution (inherited from the eruption column); vi) particles sediment from the bottom of the spreading current where turbulence diminishes and the vertical velocity is negligible, the total mass of particles, M_i (kg), of a given size fraction (having a terminal v_i) carried by the spreading current beyond a certain distance x is:

$$M_i(x;v_i) = M_0(v_i)\exp\left(-\int_{x_O}^{x}\frac{v_i w}{Q}dx\right) \tag{A.1}$$

where $M_0(v_i)$ is the initial mass of particles injected into the current at H_b having terminal velocity v_i, w is the maximum cross-wind width of the current at the source, Q is the volumetric flow rate into the current at the neutral buoyancy level, and x_0 is the plume-corner position. For sake of simplicity, in the derivation, we will not consider effects of wind and assume that the distance x is directly proportional to the square root of the isopach areas. Therefore, considering the entire range of particle terminal velocities, the total mass carried by the spreading current beyond a certain distance x is:

$$M_{Tot}(x) = \int_{v_{min}}^{v_{max}} M_i(x;v_i)dv_i = \int_{v_{min}}^{v_{max}} M_0(v_i)\exp\left(-\int_{x_O}^{x}\frac{v_i w}{Q}dx\right)dv_i \tag{A.2}$$

According to the first mean value theorem for integration there exist $v_* \in (v_{min}, v_{max})$ such that:

$$\begin{aligned} M_{Tot}(x) &= \exp\left(-\int_{x_0}^{x}\frac{v_* w}{Q}dx\right)\int_{v_{min}}^{v_{max}} M_0(v_i)dv_i \\ &= M_{0,tot}\exp\left(-\int_{x_0}^{x}\frac{v_* w}{Q}dx\right) \end{aligned} \tag{A.3}$$

Physically v_* would represent an effective mean terminal velocity of the mixture particles up to the distance x. If we make the general assumption that $v_* w/Q$ follows a power law with the distance such that:

$$v_* w/Q = kx^m \tag{A.4}$$

for a generic positive m (generalizing the assumptions made by Bursik et al. 1992), we have:

$$\begin{aligned} M_{Tot}(x) &= M_{0,tot}\exp\left[-\frac{k}{m+1}\left(x^{m+1}-x_0^{m+1}\right)\right] \\ &\equiv M_{0,\mathrm{tot}}\exp\left[-C\left(x^n-x_0^n\right)\right] \end{aligned} \tag{A.5}$$

with $C = \frac{k}{m+1}$ and $n = m + 1$ Hence the mass accumulated on the ground till the distance x can be written as:

$$M_G(x) = M_{0,tot}\left\{1-\exp\left[-C\left(x^n-x_0^n\right)\right]\right\} = \rho_{dep} V_{0,tot}\left\{1-\exp\left[-C\left(x^n-x_0^n\right)\right]\right\} \quad (A.6)$$

that at distances where $x/x_0 \gg 1$ is formally equivalent to the Weibull distribution empirically proposed by Bonadonna and Costa (2012):

$$M_G(x) = \rho_{dep} V(x) = \rho_{dep} V_{0,tot}\left\{1-\exp\left[-\left(x/\lambda\right)^n\right]\right\} \quad (A.7)$$

with $C=(1/\lambda)^n$ Note that the same derivation can be made for each given size fraction having a terminal v_i, that implies that mass distribution of each particle accumulated on the ground class follows a Weibull distribution.

Appendix 2

Table 4 Weibull parameters associated with the eruptions considered in our study that are not reported in Table 1 of main text. θ_{th}, θ_{ML}, and $\theta_{Md\phi}$ are expressed in centimeter, while n_{th}, n_{ML}, and $n_{Md\phi}$ are dimensionless. References are in caption of Table 1

#	Eruption	θ_{th}	n_{th}	θ_{ML}	n_{ML}	$\theta_{Md\phi}$	$n_{Md\phi}$
1	Vesuvius 512 (U7)	52.5	0.8	3.0	1.9		
2	Averno2-A1	55.9	1.8	5.0	1.7		
3	Averno2-A3	302.4	1.1	8.9	2.0		
4	Averno2-A4	385.6	0.8	3.0	1.4		
5	Averno2-A5	88.3	1.5	6.8	1.4		
6	Averno2-A2	194.7	2.0	6.9	1.6		
7	Boqueron C	163.8	1.0	1.3	1.2		
8	Vesuvius 512 (U5top)	42.1	1.9	3.7	2.0		
9	Montaña Blanca	4.5	0.7	1.5	1.3		
10	El Chichon A	8.4	1.0	1.9	1.1		
11	Fogo A	42.9	1.0	11.0	0.7		
12	Fogo 1563	162.1	1.3	5.7	0.7		
13	Agnano M Spina (B1)	41.3	1.7	3.0	1.7		
14	Cotopaxi L3	192.0	1.7	6.8	1.5	0.6	1.0
15	Agnano M Spina (D1)	21.5	1.8	5.0	1.8		
16	Cotopaxi L5	74.9	1.2	6.7	1.8	1.0	1.7
17	Hatepe 186 AD	21.3	1.5	4.3	1.3	0.4	1.1
18	Tarawera 1886	96.6	1.6	4.8	1.5	0.5	1.7
19	Pululagua 2450BP	56.2	1.7	1.9	2.0	0.3	1.0
20	Fontana Lapilli E	9.2	0.7	3.8	2.0		
21	Fontana Lapilli F	9.2	0.7	6.0	2.0		
22	Novarupta A 1912	11.2	0.9	13.6	0.9		
23	Novarupta C 1912	26.1	0.8	10.7	1.8		
24	Novarupta F 1912	6.6	1.0	11.2	2.0		
25	Quizapu 1932	3.4	0.5	3.1	0.7		
26	Santa Maria 1902	45.7	1.6	7.9	1.5		
27	Pinatubo 1991	3.3	1.2	3.1	1.8		
28	Minoan 3.6 ka BP	31.2	1.6	3.0	1.2		
29	Taupo 186 AD	36.7	1.5	6.4	1.0	1.4	1.2
30	Waimihia	29.6	0.4	4.6	1.3	0.7	1.4

References

Ablay GJ, Ernst GGJ, Marti J, Sparks RSJ (1995) The similar-to-2 Ka Subplinian eruption of Montana-Blanca, Tenerife. Bull Volcanol 57(5):337–355

Andronico D, Cristaldi A, Scollo S (2008a) The 4–5 September 2007 lava fountain at South-East Crater of Mt Etna, Italy. J Volcanol Geotherm Res 173(3–4):325–328

Andronico D, Scollo S, Caruso S, Cristaldi A (2008b) The 2002–03 Etna explosive activity: tephra dispersal and features of the deposits. J Geophys Res. doi:10.1029/2007JB005126

Arrighi S, Principe C, Rosi M (2001) Violent strombolian and subplinian eruptions at Vesuvius during post-1631 activity. Bull Volcanol 63(2–3):126–150

Bertagnini A, Landi P, Santacroce R, Sbrana A (1991) The 1906 eruption of Vesuvius—from magmatic to phreatomagmatic activity through the flashing of a shallow depth hydrothermal system. Bull Volcanol 53(7):517–532

Biass S, Bonadonna C (2011) A quantitative uncertainty assessment of eruptive parameters derived from tephra deposits: the example of two large eruptions of Cotopaxi volcano, Ecuador. Bull Volcanol 73(1):73–90

Bonadonna C, Costa A (2012) Estimating the volume of tephra deposits: a new simple strategy. Geology 40(5):415–418

Bonadonna C, Costa A (2013) Modeling of tephra sedimentation from volcanic plumes. In: Fagents S, Gregg T, Lopes R (eds) Modeling volcanic processes: the physics and mathematics of volcanism. Cambridge University Press, Cambridge, pp 173–202

Bonadonna C, Houghton BF (2005) Total grainsize distribution and volume of tephra-fall deposits. Bull Volcanol 67:441–456

Bonadonna C, Phillips JC (2003) Sedimentation from strong volcanic plumes. J Geophys Res 108(B7):2340–2368

Bonadonna C, Ernst GGJ, Sparks RSJ (1998) Thickness variations and volume estimates of tephra fall deposits: the importance of particle Reynolds number. J Volcanol Geotherm Res 81(3–4):173–187

Bonadonna C, Phillips JC, Houghton BF (2005) Modeling tephra sedimentation from a Ruapehu weak plume eruption. J of Geophys Res. doi:10.1029/2004JB003515

Bonadonna C, Genco R, Gouhier M, Pistolesi M, Cioni R, Alfano F, Hoskuldsson A, Ripepe M (2011) Tephra sedimentation during the 2010 Eyjafjallajokull eruption (Iceland) from deposit, radar, and satellite observations. J Geophys Res-Sol Ea. doi:10.1029/2011JB008462

Bonadonna C, Cioni R, Pistolesi M, Connor CB, Scollo S, Pioli L, Rosi M (2013) Determination of the largest clast sizes of tephra deposits for the characterization of explosive eruptions: a study of the IAVCEI commission on tephra hazard modelling. B Volcanol. doi:10.1007/s00445-012-0680-3

Bond A, Sparks RSJ (1976) The Minoan eruption of Santorini, Greece. J Geol Soc 132:1–16

Booth B, Croasdale R, Walker GPL (1978) A quantitative study of five thousand years of volcanism on Sao Miguel, Azores. Philos Trans R Soc Lond 288(1352):271–319

Branca S, Del Carlo P (2005) Types of eruptions of Etna volcano AD 1670–2003: implications for short-term eruptive behaviour. Bull Volcanol 67(8):732–742

Brown WK, Wohletz KH (1995) Derivation of the Weibull distribution based on physical principles and its connection to the Rosin-Rammler and the lognormal distributions. J Appl Phys 78:2758–2763

Bursik MI, Sparks RSJ, Gilbert JS, Carey SN (1992) Sedimentation of tephra by volcanic plumes: I. Theory and its comparison with a study of the Fogo A plinian deposit, Sao Miguel (Azores). Bull Volcanol 54:329–344

Carey SN, Sigurdsson H (1986) The 1982 eruptions of El Chichon volcano, Mexico (2): observations and numerical modelling of tephra-fall distribution. Bull Volcanol 48:127–141

Carey S, Sigurdsson H (1987) Temporal variations in column height and magma discharge rate during the 79 AD eruption of Vesuvius. Geol Soc Am Bull 99(2):303–314

Carey S, Sigurdsson H (1989) The intensity of Plinian eruptions. Bull Volcanol 51:28–40

Carey SN, Sparks RSJ (1986) Quantitative models of the fallout and dispersal of tephra from volcanic eruption columns. Bull Volcanol 48:109–125

Cashman K (2004) Volatile controls on ascent and eruption. In: Sparks RSJ, Hawkesworth CJ (eds) The state of the planet: Frontiers and challenges in geophysics: American Geophysical Union Geophysical Monograph 150, pp. 109–124

Cioni R, Sulpizio R (1998) Le sottopopolazioni granulometriche nei depositi vulcanici di caduta : l'eruzione delle pomici di Avellino (Vesuvio, Italia). Atti della societa toscana di scienze naturali residente in Pisa, memorie 105(serie A):81–97

Cioni R, Bertagnini A, Santacroce R, Andronico D (2008) Explosive activity and eruption scenarios at Somma-Vesuvius (Italy): towards a new classification scheme. J Volcanol Geotherm Res 178(3):331–346

Cioni R, Bertagnini A, Andronico D, Cole PD, Mundula F (2011) The 512 AD eruption of Vesuvius: complex dynamics of a small scale subplinian event. Bull Volcanol 73(7):789–810

Cole PD, Smith P, Komorowski JC, Alfano F, Bonadonna C, Stinton A, Christopher T, Odbert H, Loughlin S (2013, in press) Ash venting occurring both prior to and during lava extrusion at Soufrière Hills volcano, Montserrat, from 2005 to 2010. In: al. We (ed) The eruption of the Soufriere Hills Volcano, Montserrat, 2000–2010, Geological Society Memoir. Geological Society, London

Costantini L, Bonadonna C, Houghton BF, Wehrmann H (2009) New physical characterization of the Fontana Lapilli basaltic Plinian eruption, Nicaragua. Bull Volcanol 71(3):337–355

de Vita S, Orsi G, Civetta L, Carandente A, D'Antonio M, Deino A, di Cesare T, Di Vito MA, Fisher RV, Isaia R, Marotta E, Necco A, Ort M, Pappalardo L, Piochi M, Southon J (1999) The Agnano-Monte Spina eruption (4100 years BP) in the restless Campi Flegrei caldera (Italy). J Volcanol Geotherm Res 91(2–4):269–301

Degruyter W, Bonadonna C (2012) Improving on mass flow rate estimates of volcanic eruptions. Geophys Res Lett. doi:10.1029/2012GL052566

Di Vito MA, Arienzo I, Braia G, Civetta L, D'Antonio M, Di Renzo V, Orsi G (2011) The Averno 2 fissure eruption: a recent small-size explosive event at the Campi Flegrei Caldera (Italy). Bull Volcanol 73(3):295–320

Eychenne J, Le Pennec J-L (2012) Sigmoidal particle density distribution in a subplinian scoria fall deposit. Bull Volcanol 74(10):2243–2249

Fierstein J, Hildreth W (1992) The plinian eruptions of 1912 at Novarupta, Katmai National Park, Alaska. Bull Volcanol 54:646–684

Fierstein J, Nathenson M (1992) Another look at the calculation of fallout tephra volumes. Bull Volcanol 54:156–167

Fierstein J, Nathenson M (1993) Another look at the calculation of fallout tephra volumes—reply. Bull Volcanol 55(5):375–378

Fisher RV, Schmincke HU (1984) Pyroclastic rocks. Springer, Berlin, p 472

Folch A, Costa A, Basart S (2012) Validation of the FALL3D ash dispersion model using observations of the 2010 Eyjafjallajokull volcanic ash clouds. Atmos Environ 48:165–183

Garcia O, Bonadonna C, Marti J, Pioli L (2012) The 5,660 yBP Boqueron explosive eruption, Teide-Pico Viejo complex, Tenerife. Bull Volcanol 74(9):2037–2050

Gonzalez-Mellado AO, De la Cruz-Reyna S (2010) A simple semi-empirical approach to model thickness of ash-deposits for different eruption scenarios. Nat Hazard Earth Syst 10(11):2241–2257

Gudmundsson MT, Thordarson T, Hoskuldsson A, Larsen G, Bjornsson H, Prata FJ, Oddsson B, Magnusson E, Hognadottir T, Petersen GN, Hayward CL, Stevenson JA, Jonsdottir I (2012) Ash generation and distribution from the April–May 2010 eruption of Eyjafjallajokull. Scientific Reports, Iceland. doi:10.1038/srep00572, 2

Gurioli L, Harris AJL, Houghton BF, Polacci M, Ripepe M (2008) Textural and geophysical characterization of explosive basaltic activity at Villarrica volcano. J Geophys Res-Sol Ea. doi:10.1029/2007JB005328

Gurioli L, Harris AJL, Colò L, Bernard J, Favalli M, Ripepe M, Andronico D (2013, in press) Classification, landing distribution, and associated flight parameters for a bomb field emplaced during a single major explosion at Stromboli, Italy. Geology

Hildreth W, Drake RE (1992) Volcano Quizapu, Chilean Andes. Bull Volcanol 54:93–125

Holasek RE, Self S, Woods AW (1996) Satellite observations and interpretation of the 1991 Mount Pinatubo eruption plumes. J Geophys Res-Sol Ea 101(B12):27635–27655

Houghton BF, Gonnermann HM (2008) Basaltic explosive volcanism: constraints from deposits and models. Chemie Der Erde-Geochemistry 68(2):117–140

Inman DL (1952) Measures for describing the size distribution of sediments. J Sediment Petrol 22:125–145

Koyaguchi T (1996) Volume estimation of tephra-fall deposits from the June 15, 1991, eruption of Mount Pinatubo by theoretical and geological methods. In: Newhall CG, Punongbayan RS (eds). Fire and mud. Seattle: University of Washington and Quezon City: Phivolcs, p 583–600

Legros F (2000) Minimum volume of a tephra fallout deposit estimated from a single isopach. J Volcanol Geotherm Res 96:25–32

Longchamp C, Bonadonna C, Bachmann O, Skopelitis A (2011) Characterization of tephra deposits with limited exposure: the example of the two largest explosive eruptions at Nisyros volcano (Greece). Bull Volcanol 73(9):1337–1352

Marchetti E, Ripepe M, Harris AJL, Delle Donne D (2009) Tracing the differences between Vulcanian and Strombolian explosions using infrasonic and thermal radiation energy. Earth Planet Sci Lett 279(3–4):273–281

Mason BG, Pyle DM, Oppenheimer C (2004) The size and frequency of the largest explosive eruptions on Earth. Bull Volcanol 66(8):735–748

Mastin LG, Guffanti M, Servranckx R, Webley P, Barsotti S, Dean K, Durant A, Ewert JW, Neri A, Rose WI, Schneider D, Siebert L, Stunder B, Swanson G, Tupper A, Volentik A, Waythomas CF (2009) A multidisciplinary effort to assign realistic source parameters to models of volcanic ash-cloud transport and dispersion during eruptions. J Volcanol Geotherm Res 186(1–2):10–21

Mueller S, Scheu B, Kueppers U, Spieler O, Richard D, Dingwell DB (2011) The porosity of pyroclasts as an indicator of volcanic explosivity. J Volcanol Geotherm Res 203(3–4):168–174

Newhall CG, Punongbayan RS (eds) (1996) Fire and mud—eruptions and lahars of Mount Pinatubo. Philippine Institute of Volcanology and Seismology and the University of Washington Press, Philippines, p 1126p

Newhall CG, Self S (1982) The Volcanic Explosivity Index (VEI)—an estimate of explosive magnitude for historical volcanism. J Geophys Res Oceans Atm 87:1231–1238

Norini G, De Beni E, Andronico D, Polacci M, Burton M, Zucca F (2009) The 16 November 2006 flank collapse of the south-east crater at Mount Etna Italy: study of the deposit and hazard assessment. J Geophys Res-Sol Earth. doi:10.1029/2008JB005779

Oddsson B, Gudmundsson MT, Larsen G, Karlsdottir S (2012) Monitoring of the plume from the basaltic phreatomagmatic 2004 Grimsvotn eruption—application of weather radar and comparison with plume models. Bull Volcanol 74(6):1395–1407

Patrick MR, Harris AJL, Ripepe M, Dehn J, Rothery DA, Calvari S (2007) Strombolian explosive styles and source conditions: insights from thermal (FLIR) video. Bull Volcanol 69(7):769–784

Pfeiffer T, Costa A, Macedonio G (2005) A model for the numerical simulation of tephra fall deposits. J Volcanol Geo Res 140:273–294

Pioli L, Azzopardi BJ, Cashman KV (2009) Controls on the explosivity of scoria cone eruptions: magma segregation at conduit junctions. J Volcanol Geotherm Res 186(3–4):407–415

Pyle DM (1989) The thickness, volume and grainsize of tephra fall deposits. Bull Volcanol 51(1):1–15

Pyle DM (1990) New estimates for the volume of the Minoan eruption. In: Hardy DA (ed) Thera and the Aegean World. The Thera Foundation, London, pp 113–121

Pyle DM (1995) Assessment of the minimum volume of tephra fall deposits. J Volcanol Geotherm Res 69(3–4):379–382

Pyle DM (1999) Widely dispersed Quaternary tephra in Africa. Global Planet Change 21:95–112

Pyle DM (2000) Sizes of volcanic eruptions. In: Sigurdsson H, Houghton B, McNutt S, Rymer H, Stix J (eds) Encyclopedia of volcanoes. Academic, New York, p 1417

Ripepe M, Rossi M, Saccorotti G (1993) Image-processing of explosive activity at Stromboli. J Volcanol Geotherm Res 54(3–4):335–351

Rose WI (1993) Comment on another look at the calculation of fallout tephra volumes. Bull Volcanol 55(5):372–374

Rose WI, Durant AJ (2009) Fine ash content of explosive eruptions. J Volcanol Geotherm Res 186(1–2):32–39

Rosi M, Paladio-Melosantos ML, Di Muro A, Leoni R, Bacolcol T (2001) Fall vs flow activity during the 1991 climactic eruption of Pinatubo volcano (Philippines). Bull Volcanol 62:549–566

Rosi M, Pistolesi M, Bertagnini A, Landi P, Pompilio M, Di Roberto A (2013) Stromboli Volcano, Aeolian Islands (Italy): present eruptive activity and hazard. In: Lucchi F, Peccerillo A, Keller J, Tranne CA, Rossi PL (eds) Geology of the Aeolian Islands (Italy). Geological Society of London, Memoirs.

Rust AC, Cashman KV (2011) Permeability controls on expansion and size distributions of pyroclasts. J Geophy Res-Sol Ea. doi:10.1029/2011JB008494

Schneider D, Rose W, Coke L, Bluth G (1999) Early evolution of a stratospheric volcanic eruption cloud as observed with TOMS and AVHRR. J Geophys Res 104(D4):4037–4050

Scollo S, Del Carlo P, Coltelli M (2007) Tephra fallout of 2001 Etna flank eruption: analysis of the deposit and plume dispersion. J Volcanol Geotherm Res 160(1–2):147–164

Self S, Sparks RSJ (1978) Characteristics of pyroclastic deposits formed by the interaction of silicic magma and water. Bulletin Volcanologique 41:196–212

Self S, Sparks RSJ, Booth B, Walker GPL (1974) 1973 Heimaey Strombolian scoria deposit, Iceland. Geol Mag 3(6):539–548

Self S, Rampino MR, Newton MS, Wolff JA (1984) Volcanological study of the great Tambora eruption of 1815. Geology 12(11):659–663

Sparks RSJ, Wilson L, Sigurdsson H (1981) The pyroclastic deposits of the 1875 eruption of Askja, Iceland. Philos Trans R Soc Lond 229:241–273

Sparks RSJ, Bursik MI, Ablay GJ, Thomas RME, Carey SN (1992) Sedimentation of tephra by volcanic plumes. 2. Controls on thickness and grain-size variations of tephra fall deposits. Bull Volcanol 54(8):685–695

Sparks RSJ, Bursik MI, Carey SN, Gilbert JS, Glaze LS, Sigurdsson H, Woods AW (1997) Volcanic plumes. Wiley, Chichester, p 574

Sulpizio R (2005) Three empirical methods for the calculation of distal volume of tephra-fall deposits. J Volcanol Geotherm Res 145(3–4):315–336

Sulpizio R, Cioni R, Di Vito MA, Mele D, Bonasia R, Dellino P (2010) The Pomici di Avellino eruption of Somma–Vesuvius (3.9 ka BP) part I: stratigraphy, compositional variability and eruptive dynamics. Bull Volcanol. doi:10.1007/s00445-009-0339-x

Thorarinsson S (1954) The eruptiom of Hekla 1947–1948. In: The tephra fall from Hekla. Vis Islendinga, Reykjavik, p 68

Tsunematsu K (2012) New numerical solutions for the description of volcanic particle dispersal. PhD Dissertation; University of Geneva

Volentik ACM, Bonadonna C, Connor CB, Connor LJ, Rosi M (2010) Modeling tephra dispersal in absence of wind: insights from the climactic phase of the 2450 BP Plinian eruption of Pululagua volcano (Ecuador). J Volcanol Geotherm Res 193(1–2):117–136

Walker GPL (1973) Explosive volcanic eruptions—a new classification scheme. Geol Rundsch 62:431–446

Walker GPL (1980) The Taupo Pumice: product of the most powerful known (Ultraplinian) eruption? J Volcanol Geotherm Res 8:69–94

Walker GPL (1981a) Characteristics of two phreatoplinian ashes, and their water-flushed origin. J Volcanol Geotherm Res 9:395–407

Walker GPL (1981b) The Waimihia and Hatepe plinian deposits from the rhyolitic Taupo Volcanic Centre. New Zeal J Geol Geop 24:305–324

Walker GPL, Croasdale R (1971) Two plinian-type eruptions in the Azores. J Geol Soc Lond 127:17–55

Walker GPL, Self S, Wilson L (1984) Tarawera, 1886, New Zealand—a basaltic Plinian fissure eruption. J Volcanol Geotherm Res 21:61–78

Wehrmann H, Bonadonna C, Freundt A, Houghton BF, Kutterolf S (2006) Fontana tephra: a basaltic Plinian eruption in Nicaragua. Geological Society of America Special Paper 412: Volcanic Hazards in Central America. pp 209–223

Williams SN, Self S (1983) The October 1902 Plinian eruption of Santa Maria volcano, Guatemala. J Volcanol Geotherm Res 16:33–56

Wilson L, Walker GPL (1987) Explosive volcanic-eruptions.6. Ejecta dispersal in Plinian eruptions—the control of eruption conditions and atmospheric properties. Geophys J Roy Astron Soc 89(2):657–679

Wright JV, Smith AL, Self S (1980) A working terminology of pyroclastic deposits. J Volcanol Geotherm Res 8(2–4):315–336